Refinement of Austenite Grain in Carbon Steel by Addition of Titanium and Boron

Masayoshi SASAKI, Kenichi OHSASA, Masayuki KUDOH and Kiyotaka MATSUURA

Division of Materials Science and Engineering, Hokkaido University, Kita 13 Nishi 8, Kita-ku, Sapporo, Hokkaido 060-8628 Japan.

(*Received on August 24, 2007; accepted on October 30, 2007*)

The effects of the addition of titanium and boron on the austenite grain refinement in as-cast S45C carbon steel have been investigated and the results have been discussed based on an Fe–TiB_2 pseudo-binary phase diagram. The molar ratio of the added titanium and boron was fixed at 1 : 2 and the estimated molar percent of the added TiB_2 was varied from 0 to 0.5. The average austenite grain diameter decreased from 1 900 to 250 μm as the TiB_2 addition increased from 0 to 0.2 mol%, when the cooling rate was 0.02 K/s. The austenite grain diameter, however, did not exhibit further decrease when the TiB_2 addition increased from 0.2 to 0.5 mol%. The lower limit grain diameter of 250 μm was very close to the secondary dendrite arm spacing, which was not affected by the addition of titanium and boron. When the cooling rate of the molten steel increased, the grain size and the dendrite arm spacing decreased. For all cooling rates, the lower limit grain size was very close to the secondary dendrite arm spacing. Metallographic observations revealed that one austenite grain included many dendrite arms when titanium and boron was not added, while with the addition of these elements one dendrite arm included several austenite grains having the dimension of the dendrite arm diameter. It was suggested that TiB_2 particles and other inclusions such as TiC and Fe_2B were formed in the inter-dendritic positions during and after solidification and they controlled the grain boundary migration in the inter-dendritic positions.

KEY WORDS: carbon steel; solidification; phase transformation; austenite grain; grain refinement.

1. Introduction

It is known that austenite (γ) grain of carbon steel is coarsened during cooling after casting, and the grain size reaches to several millimeters. The coarsened γ grains often lead to surface cracking of continuously cast slabs and have harmful effects on the behavior of hot plastic deformation.[1)] In the case of direct rolling, γ grain structure in cast slabs is the initial structure in ausforming process.[2)] Additionally, it is known that γ structure is important because it affects the final structure of α-ferrite or pearlite structure. The refinement of γ grains is effective in α-ferrite grain refinement.[3)] Therefore the refinement of γ grain is important in casting and plastic deformation of steel.

The present authors focused on an Fe–TiB_2 pseudo-binary equilibrium diagram shown in **Fig. 1**[4)] because of two aspects. First, the starting and ending temperatures of δ/γ transformation decrease with the increase in concentration of TiB_2. It was reported that γ grains grow rapidly after the coexisting phases such as δ-ferrite or liquid phases disappear and γ becomes single phase.[5)] Therefore, the decrease in ending temperature of δ/γ transformation is expected to reduce the γ grain growth.[6)] Secondly, this alloy system has a eutectic reaction of $L \rightarrow \delta + TiB_2$ and the precipitation of TiB_2 phase from δ phase. Since the eutectic reaction and precipitation occurs before the δ/γ transformation, it is also expected that the γ grain growth is retarded by the presence of the TiB_2 phase.

This work was carried out to investigate the effects of the addition of titanium and boron on γ grain size of carbon steel.

2. Experimental Procedure

Commercial S45C steel rods having a 20 mm diameter were used as a sample material, and titanium and boron were added to this material to generate TiB_2 particles as the pinning agent. The molar ratio of the added titanium and

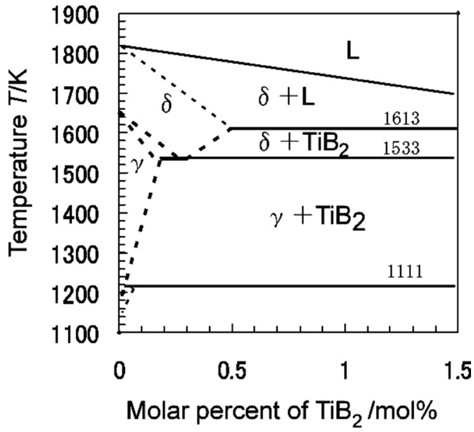

Fig. 1. Fe–TiB_2 pseudo-binary equilibrium phase diagram.[4)]

boron was 1 : 2 and the estimated molar percent of TiB_2 was varied from 0 to 0.5. Phosphorus was also added by 0.02 mass% to reveal dendritic solidification structure. The total weight of the sample was about 130 g. The sample was placed in an alumina crucible having a 35 mm inner diameter and a 45 mm depth, and was melted in a SiC electric furnace filled with argon gas of a purity higher than 99.999%.

The sample was held at 1 823 K for 1 h for melting, and then the sample was cooled down to 1 373 K at a rate between 0.02 and 2.25 K/s. At this temperature, the sample was quenched by dropping it into strongly swirling iced water.

The quenched sample was longitudinally sectioned and polished. The dendritic solidification structure and the austenite grain structure were revealed by using Oberhoffer's etchant and a 0.2% natal, respectively. The dendrite arm spacing (DAS) and the area equivalent diameter (AED) of the austenite grain were measured using an optical microscope. Scanning electron microscope (SEM) was also used to observe the fine precipitates.

3. Results and Discussion

3.1. Effect of TiB_2 Concentration

Figure 2 shows optical micrographs of austenite grain structure observed on the cross-section of the sample. The grain size of the S45C steel was extremely large (Fig. 2(a)), however the addition of titanium and boron significantly reduced the grain size (Fig. 2(b)).

Figure 3 shows the effects of the TiB_2 concentration on the AED and the DAS. It is clear that AED decreases drastically with the increase in TiB_2 concentration. However, the increase in TiB_2 concentration exceeding 0.2 mol% did not bring about further decrease in AED. The decrease was limited to approximately 250 μm. On the other hand, the DAS was not affected by the TiB_2 concentration and it was approximately 250 μm.

The fact that the decrease in AED was limited to value same as the DAS suggested that γ grains that were formed in δ-ferrite dendrite by δ/γ transformation grew within the dendrite arm area but when the grain boundary reached to the inter-arm position it was pinned there by the inclusion particles consisting of segregated elements, as shown in **Fig. 4**. To investigate whether this hypothesis is valid or not, we compared the δ-ferrite dendrite structure and γ grain structure in a same position. The results are shown in **Fig. 5**. In the case of S45C steel, as shown in Figs. 5(a) and 5(c), γ grains include some dendrite arms within them, which means that the γ grains grew across the inter-dendritic positions. On the contrary, in the case of the sample having 0.1 mol% TiB_2, as shown in Figs. 5(b) and 5(d), γ grains exist within the dendrite arms, which means that the grain growth was stopped in the inter-dendritic positions. These results strongly support the hypothesis described above. The observation using a SEM, as shown in **Fig. 6**, revealed the existence of very fine particles on the grain boundaries. It was suggested that γ grains were pinned by these very fine particles.

Analysis using EPMA indicated that most of these very fine particles were not TiB_2 but TiC or Fe_2B. Although TiB_2 particles were also detected in the present samples, most of them were large eutectic products. These eutectic TiB_2 particles were formed in the inter-dendritic positions in the samples containing high concentrations of titanium and

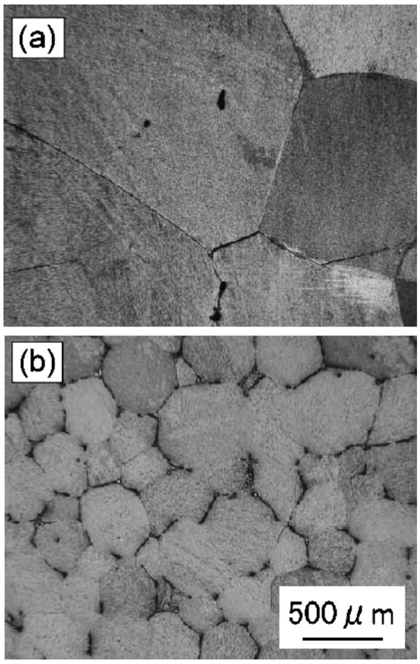

Fig. 2. Austenite grain structures of samples cooled at 0.02 K/s and quenched from 1 373 K. (a) S45C steel and (b) S45C steel with the addition of 0.2 mol% Ti and 0.4 mol% B.

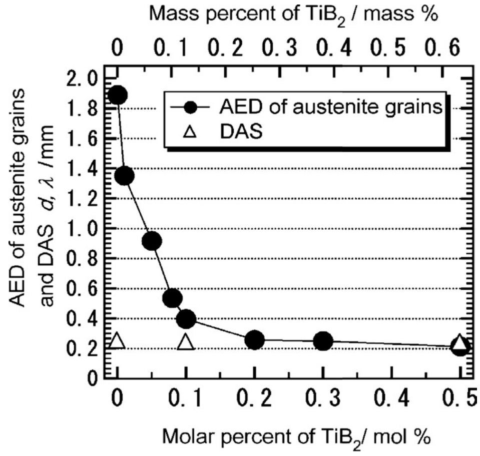

Fig. 3. Effects of TiB_2 content on the area equivalent diameter (AED) of austenite grains and the dendrite arm spacing (DAS). Cooling rate was 0.02 K/s.

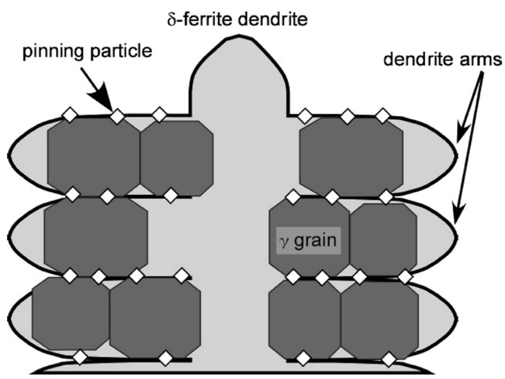

Fig. 4. Schematic of pinning effect by the inclusion particles consisting of segregated elements.

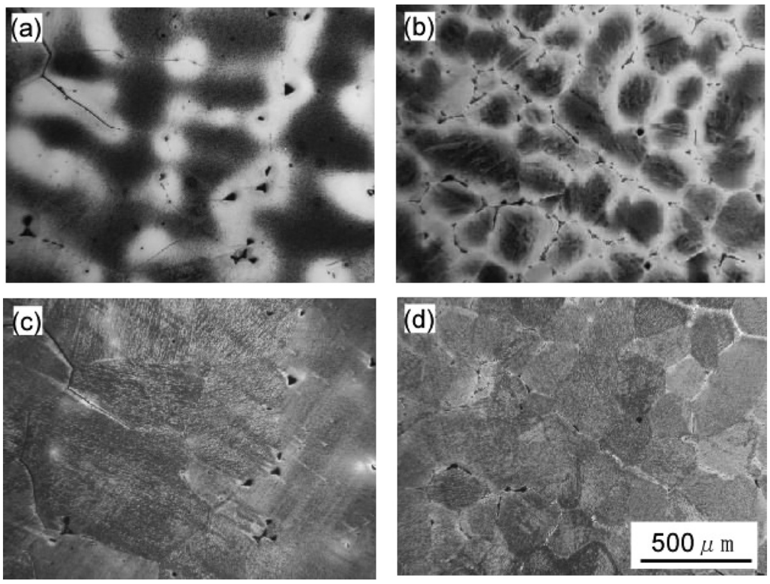

Fig. 5. Comparison between dendrite and γ grain structures at same positions. (a) and (c): S45C steel, (b) and (d): S45C steel with the addition of 0.2 mol% Ti and 0.4 mol% B.

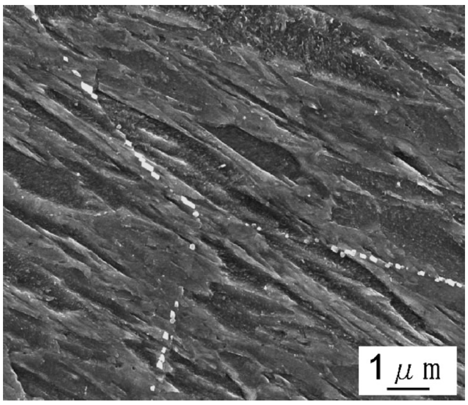

Fig. 6. Fine particles existing on γ grain boundaries. The concentration of Ti and B were 0.1 and 0.2 mol%, respectively. Cooled at 0.02 K/s.

boron, and they played a roll of "pin" to limit the grain size to a size similar to the dendrite arm spacing. The present authors have recently stared the investigation of the effects of the individual addition of titanium and boron. Although the data obtained is few at the moment, the results indicate that the individual addition is also effective in the grain refinement. In the case of individual addition of titanium and boron, the pin is considered to be TiC and FeB_2, as they were detected in the present study. The results will be reported after collecting detailed data.

3.2. Effect of Cooling Rate

We considered that since the grain refinement based on the pinning effect was limited to the grain size similar to the dendrite arm spacing, reduction in dendrite arm spacing would bring about further grain size refinement. Generally, the reduction in dendrite arm spacing can be realized by the increase in cooling rate.[7] Therefore, we investigated the relation ship between the dendrite arm spacing and grain size at higher cooling rates.

Figure 7 shows micrographs of dendrite and γ grain structures of a sample cooled at a higher rate of 2.25 K/s with the addition of titanium and boron. At this cooling rate the DAS was approximately 60 μm, which is much smaller than that of samples shown in Figs. 5(a) and 5(b). On the other hand, the γ grain size of this sample was also approximately 60 μm, which is similar to the DAS.

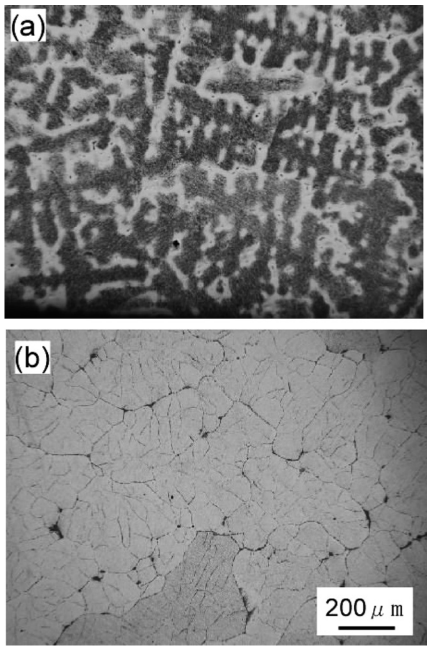

Fig. 7. Microstructures of the specimen cooled at 2.25 K/s. The concentrations of Ti and B were 0.1 and 0.2 mol%, respectively.

The effects of cooling rate on the AED of γ grains and DAS are summarized in **Fig. 8**. Both the AED and DAS decreased with the increase in cooling rate. The addition of titanium and boron of 0.1 and 0.2 mol%, corresponding to 0.1 mol% of TiB_2, significantly reduced the AED, while it did not affect the DAS. The AED was about 400 μm at a cooling rate of 0.02 K/s for the sample with the addition of the elements, while the DAS was about 250 μm for the same condition. These results indicate that the concentration of TiB_2 of 0.1 mol% is not enough for the entire con-

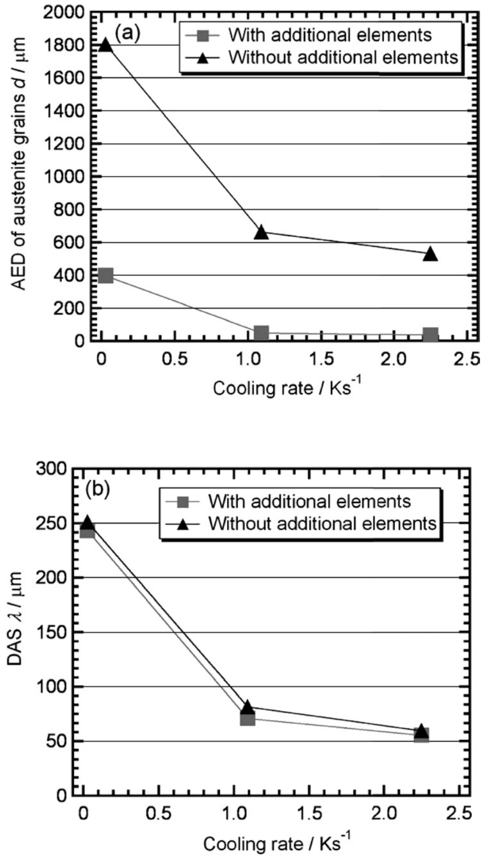

Fig. 8. Effects of cooling rate and the addition of Ti and B on the size of AED of γ grains and DAS. The concentrations of Ti and B were 0.1and 0.2 mol%, respectively.

trol of the grain boundary migration. However, when the cooling rate was higher the AED and DAS exhibited the similar values regardless of the low concentration of TiB_2. It is likely that the increase in cooling rate enhanced the segregation of the added elements at the inter-dendritic positions and TiB_2 particles and other inclusion particles formed there effectively pinned the grain boundary. The results shown in Fig. 8 strongly support the hypothesis that the growth of the γ grains are stopped at the inter-arm position due to the inclusion particles consisting of segregated elements.

4. Conclusions

The effects of the addition of titanium and boron on the austenite grain size of a commercial carbon steel of S45C was investigated. The results are summarized as follows.

(1) As the concentrations of titanium and boron increased, the austenite grain size decreased. The decrease was, however, limited to the dendrite arm spacing.

(2) As the cooling rate increased, both the dendrite arm spacing and the austenite grain size decreased. When titanium and boron were added, the dendrite spacing and the austenite grain size exhibited similar values regardless of the cooling rate.

(3) It was suggested that the austenite grains that were formed in δ-ferrite dendrite by δ/γ transformation were able to grow within the dendrite arm area but when the grain boundary reached the inter-arm position it was pinned there by the inclusion particles consisting of segregated elements.

REFERENCES

1) Y. Maehara, K. Ysumoto, Y. Sugitani and K. Gunji: *Trans. Iron Steel Inst. Jpn.*, **71**(1985), 1045.
2) N. Yoshida, Y. Kobayashi, and K. Ngai: *Tetsu-to-Hagané*, **90** (2004), No. 4.
3) M. Tadashi: *Tetsu-to-Hagané*, **87** (1995), No. 11.
4) P. Villars, A. Prince and H. Okamoto: Handbook of Ternary Alloy Phase Diagrams, Vol. 5, (1995), 5645.
5) T. Maruyama, M. Kudoh and Y. Itoh: *Tetsu-to-Hagané*, **86** (2000), No. 2.
6) K. Yasumoto, T. Nagamichi, Y. Maehara and K. Gunji: *Tetsu-to-Hagané*, **73** (1987), 1738.
7) W. Kurz and D. J. Fisher: *Acta Metall.*, **29** (1981), 11.